Supplement materials for Seasonal influence on Post-Fire Debris Flow likelihood after the 2020 Lake Fire by Chong et al., 2025

This supplementary material consists of 6 figures and 7 tables.

1. Test for dNDVI calibration and validation

We validated our dNDVI values with field observations using consistent resolution from satellite (3 x 3 meters). We identified and validated using the road and three other locations (1 unburned campsite & 2 by the river in the burned perimeter). We created another set of calibration sites on roads only to have more consistent dNDVI values than the other locations due to the absence of vegetation and greater exposure to sunlight.

We found that in some dNDVI dates, the road values have either a similar reduction/increase in dNDVI or vary across the five points. On the few dates where dNDVI values fluctuate across location pixels, we can use the mean values to subtract across the image to calibrate. However, the other dates where the different dNDVI values across the five points can be attributed to local effects (e.g., shadows, water, dust) or other processes. In this study, we were not successful in creating a standardized dNDVI calibration due to the inconsistent orbits and acquisition times from the satellite imagery and the lack of consistent field validation over long periods at the different locations.

2. Other satellite imagery processing

To determine the effectiveness of other vegetation index methods, we tested with relative NDVI (rdNDVI) in our study site. The rdNDVI method has been used to detect landslides and show the severity of debris flow changes using the relative percent change (equation 2 in Scheip and Wegmann 2021). However, in our study, there were no clear differences between rdNDVI and dNDVI. A possible reason for the lack of clear differences is the lack of the greenest-pixel composite that is needed for the pre-NDVI in our study, which requires extensive computational power and time to acquire. Moreover, our rdNDVI has values greater than -100% or 100% which could be caused by the different imaging sensors on PlanetScope as compared to Sentinel-2 or Landsat-7/8 (Scheip and Wegmann 2021). However, further analysis is also needed to understand the product of calibrating different satellite sensors with inconsistent orbits.

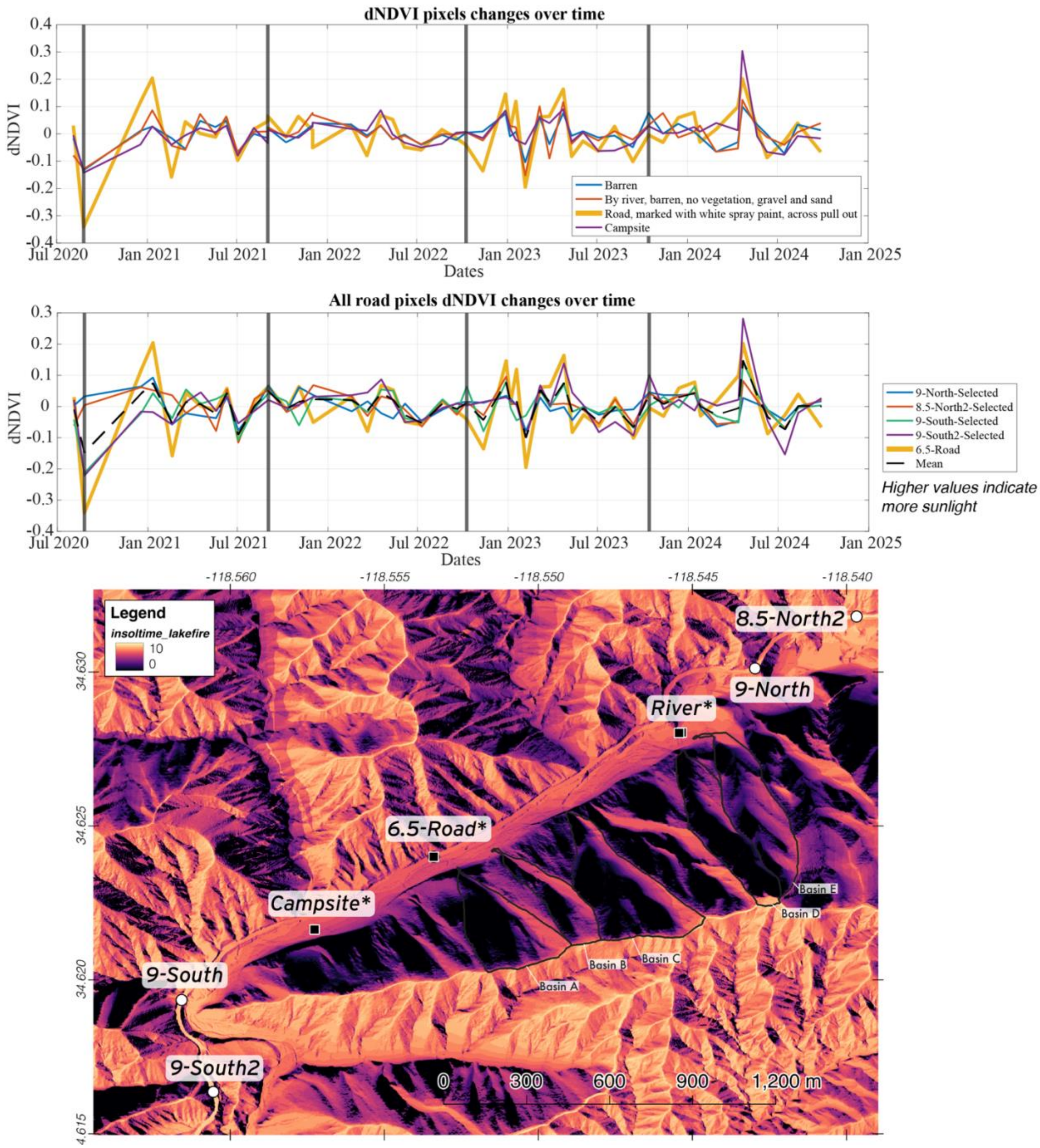

Figure S1: Top panel shows the dNDVI pixel changes across four points with field validation. Bottom panel shows the location of the road pixels from field-validated and unvalidated road pixels in a solar insolation map (hours). *indicate field validated points to check on the coverage. Values before the name are the insolation time for each road pixel.

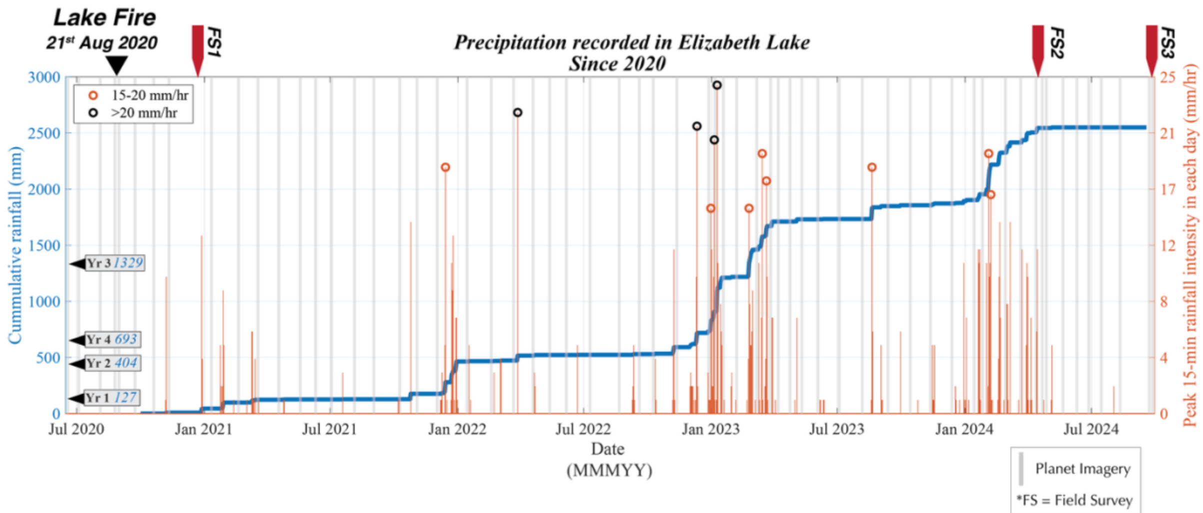

Figure S2: Record of cumulative precipitation in blue graph (blue axis) and the daily peak rain intensity (orange axis). Orange circles represent rain intensity between I_{15} of 15-20 mm/hr, and dark circles are I_{15} greater than 20 mm/hr. FS represents field survey. Grey lines represent the dates with PlanetScope images. See **Table S7** for the dates exceeding the I_{15} = 15 mm/hr.

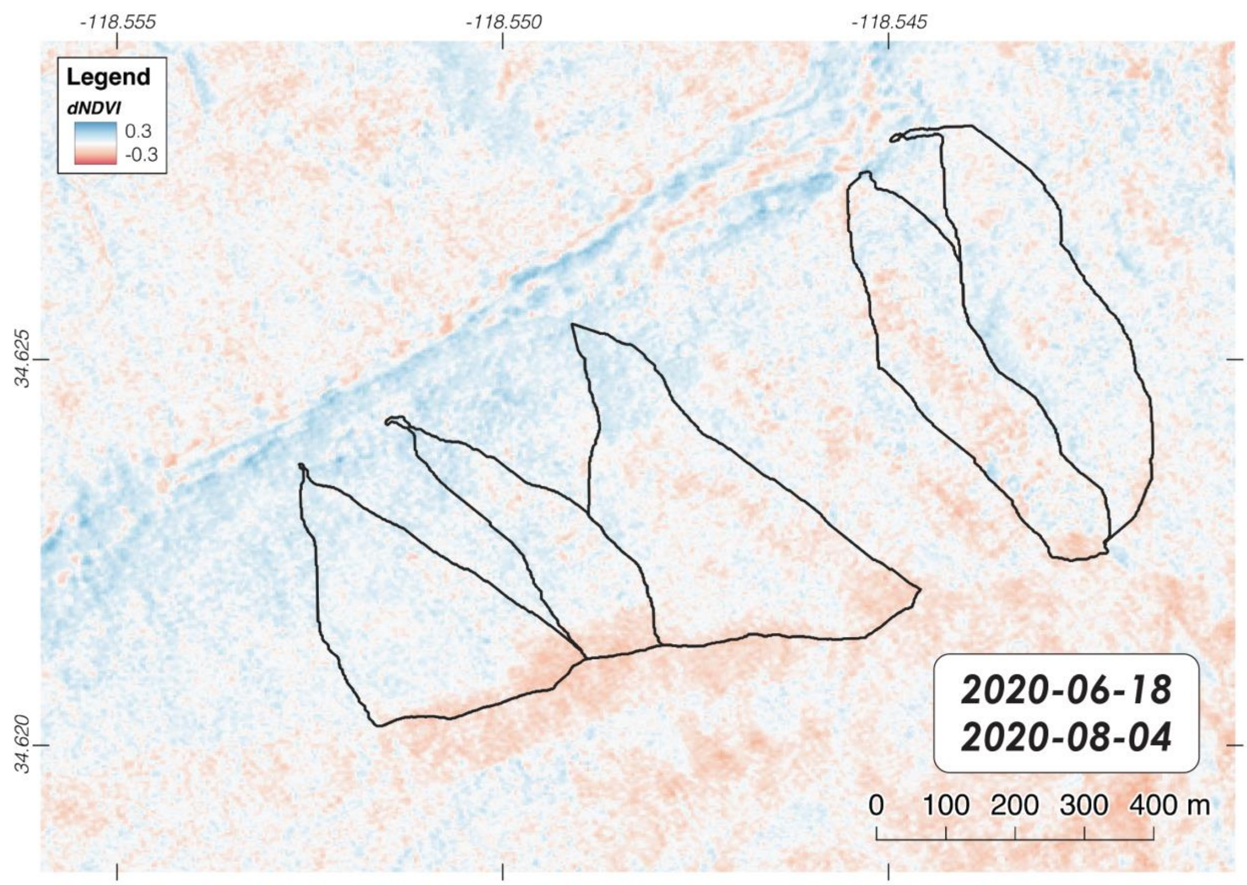

Figure S3: Pre-fire dNDVI from June 2020 to August 2020. Basins are extracted from QGIS's Channel network and drainage toolbox.

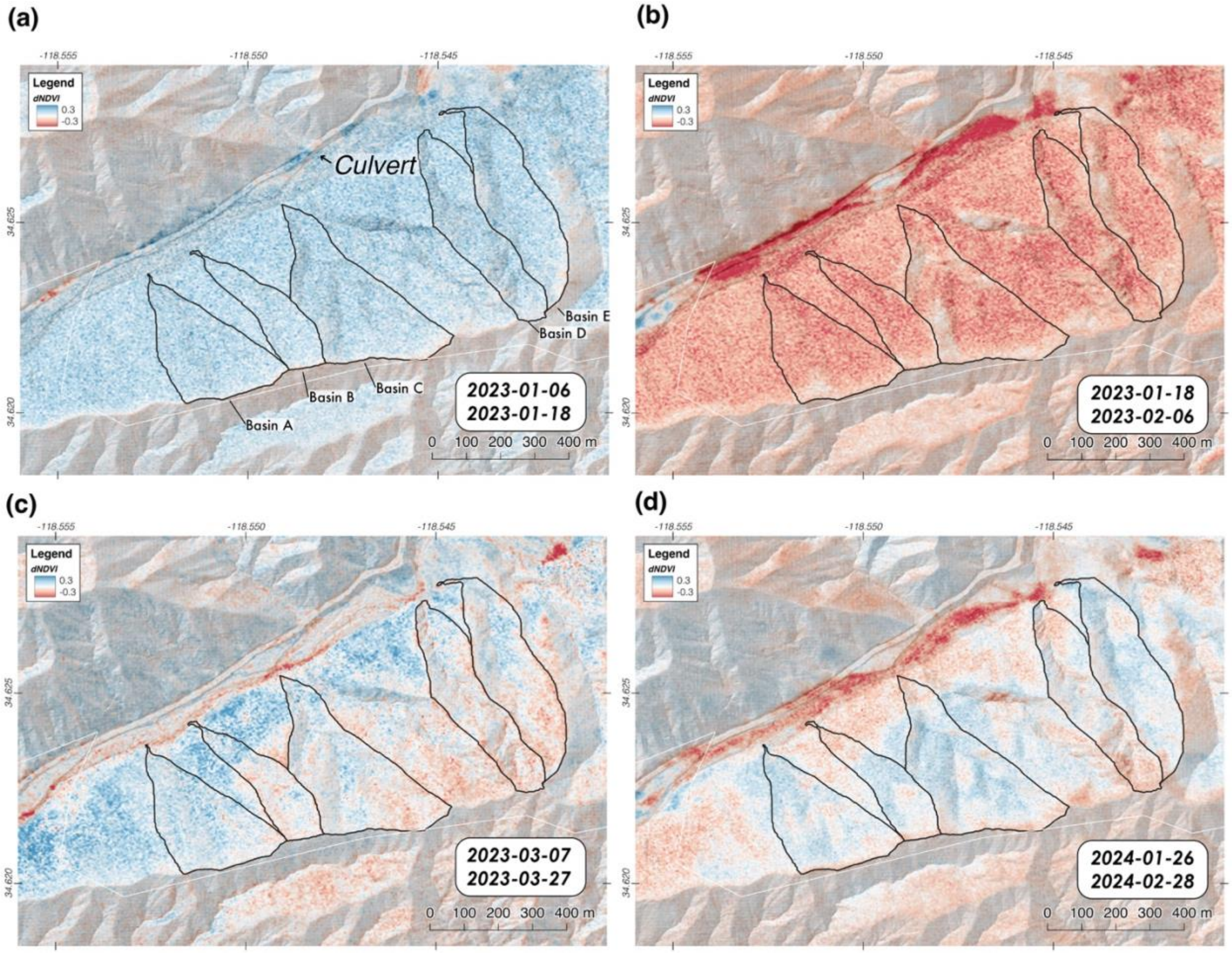

Figure S4: Selected date pairs showing dNDVI in 2023 and 2024.

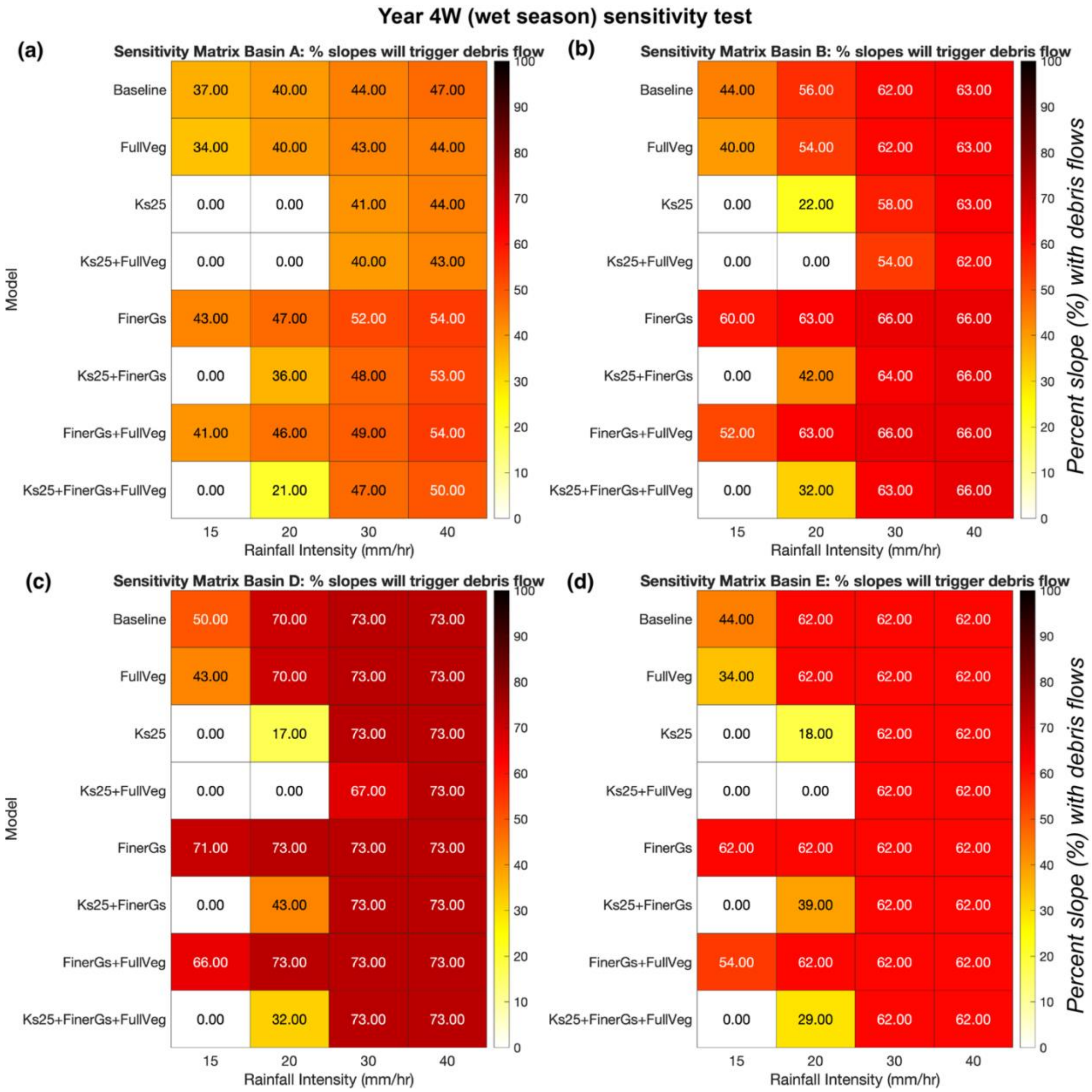

Figure S5: Sensitivity test using grain size from the 2nd field sampling. Plotted from **Table S5**.

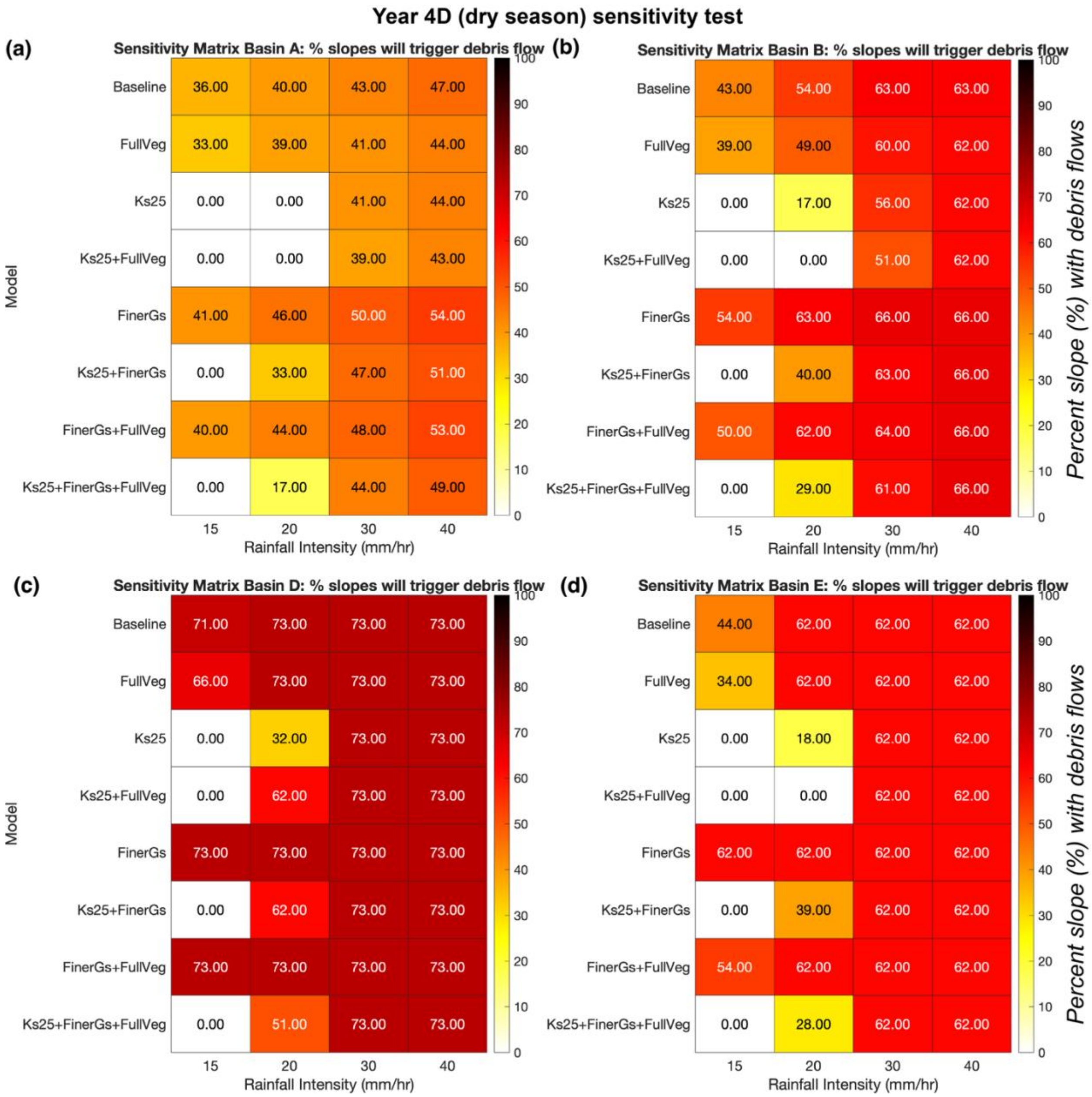

Figure S6: Sensitivity test using grain size from the 3rd field sampling. Plotted from **Table S6**.

Date	Time (UTC)	Satellite code 4-digit	ID	Notes
6/18/20	17:52:52	2304	20200618_175152_97_2304	PreFire
7/4/20	17:52:57	2277	20200704_175257_02_2277	PreFire
8/4/20	17:50:10	220b	20200804_175010_87_220b	PreFire
8/25/20	17:53:50	2304	20200825_175350_53_2304	PostFire; dNDVI yearly
8/31/20	17:49:04	2206	20200831_174904_51_2206	PostFire
9/23/20	17:57:35	2259	20200923_175735_97_2259	PostFire
10/20/20	17:54:37	2257	20201020_175437_23_2257	PostFire
11/11/20	17:50:50	220b	20201111_175050_48_220b	PostFire
12/18/20	17:52:20	222b	20201218_175220_11_222b	Post; sample collection on 23rd Dec 2020
1/11/21	17:56:58	225a	20210111_175658_38_225a	PostFire
2/19/21	17:56:17	2233	20210219_175617_31_2233	PostFire
3/19/21	17:51:51	2428	20210319_175151_40_2428	PostFire
4/18/21	17:52:41	222b	20210418_175241_02_222b	PostFire
5/19/21	17:50:42	2445	20210519_175042_85_2445	PostFire
6/10/21	17:48:25	2444	20210610_174825_69_2444	PostFire
7/3/21	17:49:22	222b	20210703_174922_92_222b	PostFire
8/5/21	17:45:50	241b	20210805_174550_13_241b	PostFire
9/2/21	17:58:06	2251	20210902_175806_40_2251	PostFire; dNDVI yearly
10/9/21	17:47:22	2423	20211009_174722_95_2423	PostFire
11/3/21	17:46:34	242b	20211103_174634_39_242b	PostFire
12/2/21	17:44:06	2442	20211202_174406_76_2442	PostFire
1/14/22	17:48:06	2432	20220114_174806_76_2432	PostFire
2/18/22	17:45:41	2431	20220218_174541_32_2431	PostFire
3/22/22	17:43:48	245a	20220322_174348_57_245a	PostFire
4/19/22	17:43:18	2439	20220419_174318_02_2439	PostFire
5/13/22	17:40:35	2449	20220513_174035_23_2449	PostFire
6/6/22	17:42:09	241d	20220606_174209_43_241d	PostFire
7/10/22	17:39:16	2436	20220710_173916_95_2436	PostFire

8/21/22	17:40:53	2455	20220821_174053_41_2455	PostFire
9/19/22	17:41:03	2432	20220919_174103_42_2432	PostFire; dNDVI yearly
10/9/22	17:37:58	2459	20221009_173758_96_2459	PostFire
11/12/22	17:38:42	2429	20221112_173842_34_2429	PostFire
12/28/22	18:14:27	24a5	20221228_181427_50_24a5	No other 17:00UTC scenes
1/6/23	17:58:52	225a	20230106_175852_17_225a	PostFire
1/18/23	17:39	2458	20230118_173959_26_2458	PostFire
2/6/23	17:43	24b3	20230206_174355_36_24b3	PostFire
3/7/23	17:47:15	24be	20230307_174715_25_24be	Cloud present within the image
3/27/23	17:43:56	24a1	20230327_174356_21_24a1	PostFire
4/7/23	17:42:57	24b2	20230407_174257_70_24b2	PostFire
4/24/23	17:42:04	2465	20230424_174204_61_2465	PostFire
5/11/23	17:40:11	241d	20230511_174011_35_241d	PostFire
6/3/23	17:45:38	24c4	20230603_174538_06_24c4	PostFire
7/4/23	17:48:06	24bb	20230704_174806_23_24bb	PostFire
8/6/23	17:45:37	24b4	20230806_174537_35_24b4	PostFire
9/12/23	17:39:57	2451	20230912_173957_55_2451	PostFire; dNDVI yearly
10/14/23	17:50:06	24bb	20231014_175006_68_24bb	PostFire
11/12/23	17:45:49	24bf	20231112_174549_76_24bf	PostFire
12/13/23	17:50:52	24b9	20240114_175121_05_24b0	PostFire
1/14/24	17:51:21	24b0	20231213_175052_25_24b9	PostFire
1/26/24	17:51:41	24c2	20240126_175141_62_24c2	Checking after heavy January rain
2/28/24	17:51:21	2423	20240228_175123_37_2423	Checking before heavy February rain
3/21/24	17:54:15	24ca	20240321_175415_38_24ca	Month month-long rain since March
4/12/24	17:55:26	24ba	20240412_175526_58_24ba	Month month-long rain since March
4/21/24	17:57:54	2455	20240421_175754_47_2455	(2nd survey) Day of sampling: PostFire
4/27/24	17:55:27	24c9	20240427_175527_48_24c9	PostFire
5/21/24	17:54:01	24b5	20240521_175401_39_24b5	PostFire
6/10/24	17:57:06	24af	20240610_175706_05_24af	PostFire

6/27/24	17:56:59	24a1	20240627_175659_40_24a1	PostFire
7/15/24	17:55:00	24bf	20240715_175500_33_24bf	PostFire
8/11/24	17:59:27	24ce	20240811_175927_64_24ce	PostFire
9/27/24	18:03:16	24ce	20240927_180316_48_24ce	(3rd survey) Day of sampling, PostFire; dNDVI yearly

Table S1: Descriptions of the 61 Planet images downloaded for analysis.

Basins	Year since the fire	Hydraulic Conductivity (mm/hr)	Canopy Cover (fraction)	Pi (Throughfall coefficient)	D50 (mm)	D84 (mm)
A	0	10[a]	0	1*	0.66	1.77
	1	10[a]	0.57	0.43	0.66	1.77
	2	-	0.99	0.01	-	-
	3	34	0.87	0.13	0.1	0.24
	4	22	0.84	0.16	0.11	0.34
B	0	10[a]	0	1*	1.38	2.45
	1	10[a]	0.29	0.71	1.38	2.45
	2	-	0.93	0.07	-	-
	3	24	0.78	0.22	0.08	0.26
	4	405	0.93	0.07	0.09	0.39
C	0	10[a]	0	1*	0.38	0.9
	1	10[a]	0.47	0.53	0.38	0.9
	2	-	0.98	0.02	-	-
	3	-	0.86	0.14	-	-
	4	-	0.85	0.15	-	-
D	0	10[a]	0	1*	1.34	2.45
	1	10[a]	0.03	0.97	1.34	2.45
	2	-	0.97	0.03	-	-
	3	22	0.75	0.25	0.1	0.27
	4	576	0.94	0.06	0.05	0.2
E	0	10[a]	0	1*	1.02	1.77
	1	10[a]	0.26	0.74	1.02	1.77
	2	-	0.99	0.01	-	-
	3	31	0.93	0.07	0.085	0.25
	4	157	0.96	0.04	0.086	0.32

Table S2: Yearly basin properties from field measurements and satellite imagery for canopy cover. This assumes the 2nd sampling is in Year 3 and the 3rd sampling in Year 4 (not classifying as wet and dry seasons in the 4th year).

Basins	Year since the fire	Debris flow occurrence (slope) 15 mm/hr	Debris flow occurrence (slope) 20 mm/hr	Debris flow occurrence (slope) 30 mm/hr
A	0	None	None	>30
	1	None	None	>30
	2	-	-	-
	3	None	None	>26
	4	None	>45	>22
B	0	None	None	None
	1	None	None	None
	2	-	-	-
	3	None	>44	>18
	4	None	None	None
C	0	>55	>30	>27
	1	>57	>33	>29
	2	-	-	-
	3	-	-	-
	4	-	-	-
D	0	None	None	None
	1	None	None	None
	2	-	-	-
	3	None	>38	**All**
	4	None	None	None
E	0	None	>50	>45
	1	None	None	48 only
	2	-	-	-
	3	None	None	**All**
	4	None	None	None

Table S3: Table showing slopes with triggering post-fire debris flows based on properties from Table S2. This assumes the 2nd sampling is in Year 3 and the 3rd sampling in Year 4 (not classifying as wet and dry seasons in the 4th year).

Basins	Intensity	Baseline	Model1Veg	Model2Ks25	Model3Ks25Veg	Model4Gs	Model5KsGs	Model6GsVeg	Model7KsGsVeg
A	15	0.00	0.00	0.00	0.00	0.00	0.00	0.00	0.00
A	20	0.00	0.00	0.00	0.00	0.19	0.00	0.17	0.00
A	30	0.17	0.14	0.01	0.00	0.71	0.68	0.70	0.16
A	40	0.71	0.69	0.68	0.14	0.72	0.70	0.71	0.71
B	15	0.00	0.00	0.00	0.00	0.00	0.00	0.00	0.00
B	20	0.00	0.00	0.00	0.00	0.01	0.00	0.01	0.00
B	30	0.01	0.01	0.00	0.00	0.63	0.01	0.63	0.00
B	40	0.01	0.01	0.01	0.01	0.68	0.26	0.67	0.23
D	15	0.00	0.00	0.00	0.00	0.00	0.00	0.00	0.00
D	20	0.00	0.00	0.00	0.00	0.00	0.00	0.00	0.00
D	30	0.00	0.00	0.00	0.00	0.63	0.00	0.19	0.00
D	40	0.00	0.00	0.00	0.00	0.63	0.61	0.63	0.21
E	15	0.00	0.00	0.00	0.00	0.00	0.00	0.00	0.00
E	20	0.00	0.00	0.00	0.00	0.01	0.00	0.01	0.00
E	30	0.01	0.00	0.00	0.00	0.24	0.13	0.21	0.01
E	40	0.19	0.17	0.01	0.00	0.69	0.26	0.68	0.22

Table S4: Sensitivity test using grain sizes from first field sampling. Values in tables show the percentage change with slopes exceeding the threshold to cause runoff-generated debris flows. The matrix plot is shown in **Figure 6**.

Basins	Intensity	Baseline	Model1Veg	Model2Ks25	Model3Ks25Veg	Model4Gs	Model5KsGs	Model6GsVeg	Model7KsGsVeg
A	15	0.37	0.34	0.00	0.00	0.43	0.00	0.41	0.00
A	20	0.40	0.40	0.00	0.00	0.47	0.36	0.46	0.21
A	30	0.44	0.43	0.41	0.40	0.52	0.48	0.49	0.47
A	40	0.47	0.44	0.44	0.43	0.54	0.53	0.54	0.50
B	15	0.44	0.40	0.00	0.00	0.60	0.00	0.52	0.00
B	20	0.56	0.54	0.22	0.00	0.63	0.42	0.63	0.32
B	30	0.62	0.62	0.58	0.54	0.66	0.64	0.66	0.63
B	40	0.63	0.63	0.63	0.62	0.66	0.66	0.66	0.66
D	15	0.50	0.43	0.00	0.00	0.71	0.00	0.66	0.00
D	20	0.70	0.70	0.17	0.00	0.73	0.43	0.73	0.32
D	30	0.73	0.73	0.71	0.67	0.73	0.73	0.73	0.73
D	40	0.73	0.73	0.73	0.73	0.73	0.73	0.73	0.73
E	15	0.44	0.34	0.00	0.00	0.62	0.00	0.54	0.00
E	20	0.62	0.62	0.18	0.00	0.62	0.39	0.62	0.29
E	30	0.62	0.62	0.62	0.62	0.62	0.62	0.62	0.62
E	40	0.62	0.62	0.62	0.62	0.62	0.62	0.62	0.62

Table S5: Sensitivity test using grain sizes from the 2nd field sampling (Year 4W). Values in tables show the percentage change with slopes exceeding the threshold to cause runoff-generated debris flows. The matrix plot is shown in **Figure S4**.

Basins	Intensity	Baseline	Model1Veg	Model2Ks25	Model3Ks25Veg	Model4Gs	Model5KsGs	Model6GsVeg	Model7KsGsVeg
A	15	0.36	0.33	0.00	0.00	0.41	0.00	0.40	0.00
A	20	0.40	0.39	0.00	0.00	0.46	0.33	0.44	0.17
A	30	0.43	0.41	0.40	0.39	0.50	0.47	0.48	0.44
A	40	0.47	0.44	0.44	0.43	0.54	0.51	0.53	0.49
B	15	0.43	0.39	0.00	0.00	0.54	0.00	0.50	0.00
B	20	0.54	0.49	0.17	0.00	0.63	0.40	0.62	0.29
B	30	0.63	0.60	0.56	0.51	0.66	0.63	0.64	0.61
B	40	0.63	0.62	0.62	0.62	0.66	0.66	0.66	0.66
D	15	0.71	0.66	0.00	0.00	0.73	0.00	0.73	0.00
D	20	0.73	0.73	0.43	0.32	0.73	0.62	0.73	0.51
D	30	0.73	0.73	0.73	0.73	0.73	0.73	0.73	0.73
D	40	0.73	0.73	0.73	0.73	0.73	0.73	0.73	0.73
E	15	0.44	0.34	0.00	0.00	0.62	0.00	0.54	0.00
E	20	0.62	0.62	0.18	0.00	0.62	0.39	0.62	0.28
E	30	0.62	0.62	0.62	0.62	0.62	0.62	0.62	0.62
E	40	0.62	0.62	0.62	0.62	0.62	0.62	0.62	0.62

Table S6: Sensitivity test using grain sizes from the 3rd field sampling (Year 4D). Values in tables show the percentage change with slope exceeding the threshold to cause runoff-generated debris flows. The matrix plot is shown in **Figure S5**.

Dates	Rain intensity (I_{15}) (mm/hr)
14th December 2021	18.28
28th March 2022	22.35
11th December 2022	21.36
31st December 2022	15.24
5th January 2023	20.32
9th January 2023	24.38
24th February 2023	15.24
15th March 2023	19.30
21st March 2023	17.27
20th August 2023	18.28
4th February 2024	19.03
7th February 2024	16.26

Table S7: Days with rainfall intensity exceeding I_{15} = 15 mm/hr.

References

Scheip, C. M. and Wegmann, K. W.: HazMapper: a global open-source natural hazard mapping application in Google Earth Engine, Nat. Hazards Earth Syst. Sci., 21, 1495–1511, https://doi.org/10.5194/nhess-21-1495-2021, 2021.